Published in final edited form as:
Mol Cancer Res. 2014 November ; 12(11): 1547–1559. doi:10.1158/1541-7786.MCR-14-0106-T.

Glucose-6-phosphatase is a Key Metabolic Regulator of Glioblastoma Invasion

Sara Abbadi[1], **Julio J. Rodarte**[1], **Ameer Abutaleb**[3], **Emily Lavell**[1], **Chris L. Smith**[1,2], **William Ruff**[1], **Jennifer Schiller**[4], **Alessandro Olivi**[1], **Andre Levchenko**[2], **Hugo Guerrero-Cazares**[1,*], and **Alfredo Quinones-Hinojosa**[1,*]

[1]Department of Neurosurgery and Oncology, Johns Hopkins University School of Medicine, Baltimore, Maryland, USA

[2]Department of Biomedical Engineering, Johns Hopkins University School of Medicine, Baltimore, Maryland, USA (Current Address: Yale Systems Biology Institute, Yale University)

[3]University of Maryland, School of Medicine, Baltimore, Maryland, USA

[4]Brandeis University, Waltham, Massachusetts, USA

Abstract

Glioblastoma (GBM) remains the most aggressive primary brain cancer in adults. Similar to other cancers, GBM cells undergo metabolic reprogramming to promote proliferation and survival. Glycolytic inhibition is widely used to target such reprogramming. However, the stability of glycolytic inhibition in GBM remains unclear especially in a hypoxic tumor microenvironment. In this study, it was determined that glucose-6-phosphatase-α (G6PC/G6Pase) expression is elevated in GBM when compared to normal brain. Human-derived brain tumor initiating cells (BTICs) utilize this enzyme to counteract glycolytic inhibition induced by 2-Deoxy-D-glucose (2DG) and sustain malignant progression. Down-regulation of G6PC renders the majority of these cells unable to survive glycolytic inhibition, and promotes glycogen accumulation through the activation of glycogen synthase (GYS1) and inhibition of glycogen phosphorylase (PYGL). Moreover, BTICs that survive G6PC knockdown are less aggressive (reduced migration, invasion, proliferation, and increased astrocytic differentiation). Collectively, these findings establish G6PC as a key enzyme with pro-malignant functional consequences that has not been previously reported in GBM and identify it as a potential therapeutic target.

[*]Corresponding Authors: Alfredo Quinones-Hinojosa, Department of Neurosurgery and Oncology, Johns Hopkins University, 1550 Orleans St, CRB-II, Room 247A, Baltimore, MD 21201. Phone: 410-502-2869, Fax: 410-502-7559, aquinon2@jhmi.edu. Hugo Guerrero-Cazares, Department of Neurosurgery, Johns Hopkins University, 1550 Orleans St, CRB-II, Room 247B, Baltimore, MD 21201. Phone: 410-502-2869, Fax: 410-502-7559, hguerre1@jhmi.edu.

Disclosure of Potential Conflicts of Interest: The authors disclose no potential conflicts of interest or financial disclosures.

Authors' Contributions

Conception and design: S. Abbadi, H. Guerrero-Cazares, and A. Quinones-Hinojosa

Development of methodology: S. Abbadi, J.J. Rodarte

Acquisition of data: S. Abbadi, C.L. Smith, and J. Schiller tracked and analyzed migration time-lapse data. W. Ruff, J. Schiller and E. Lavell assisted with early experiments.

Analysis and interpretation of data: S. Abbadi, H. Guerrero-Cazares, J.J. Rodarte, A. Olivi, A. Levchenko, A. Quinones-Hinojosa

Writing, review and/or revision of the manuscript: S. Abbadi, H. Guerrero-Cazares, J.J. Rodarte, A. Abutaleb, E. Lavell, A. Quinones-Hinojosa

Study supervision: A. Quinones-Hinojosa

Keywords

glioblastoma; G6PC; glycogen; glycolysis; hypoxia

Introduction

Glioblastoma (GBM) is the most aggressive primary brain cancer in adults (1, 2). The diffuse infiltrative nature of GBMs makes their total surgical resection impossible, leading to poor prognosis and short survival (3). A growing body of evidence has demonstrated that cancer cells display cellular hierarchies with a subset of cells believed to be responsible for resistance to conventional cancer therapies and for promotion of tumor growth (4). In cancers originating in the brain, these cells are called brain tumor initiating cells (BTICs), cancer stem cells, or tumor propagating cells (5, 6).

The rapid expansion of GBMs and other solid tumors causes them to frequently outgrow their blood supply leading to oxygen deficiency and nutrient deprivation (7, 8). As a response, tumors undergo angiogenesis to increase their oxygen and nutrient supply (9). Anti-angiogenic therapy in solid tumors shows beneficial effects associated with a reduction of the vasculature and delayed tumor progression, but ultimately increases tumor hypoxia and induces a treatment-resistant phenotype (10). These findings which are unique to cancer cells are driven by a constant metabolic reprogramming that enhances their survival adaptation in response to hypoxia (11). One well established example of this reprogramming is the Warburg effect (preference for aerobic glycolysis), which has been of particular interest in cancer cell metabolism (12). However, the enhanced glycolysis seen with the Warburg effect cannot be completely functional under hypoxic conditions wherein nutrient supply is insufficient. Thus cancer cells may additionally activate other metabolic processes, such as glycogen mobilization, to provide intermediates for their enhanced, reprogrammed glycolytic pathway (13).

Metabolic reprogramming allows BTICs to survive and adapt to restricted nutrition conditions (14). Targeting such adaptation mechanism, which is common to most cancer cells, could be a crucial therapeutic tool (15). Previously, we demonstrated that glycolytic inhibition of BTICs with the glucose analogue 2-Deoxy-D-glucose (2DG) promoted neuronal commitment and decreased cell proliferation rate, inducing a less malignant phenotype (16). However, some BTICs are able to survive glycolytic inhibition and recover their aggressive phenotype. The precise mechanism by which BTICs counteract glycolytic inhibition remains unknown.

A key enzyme in the regulation of glucose homeostasis and the glycogenolytic pathway is the glucose-6-phosphatase complex, which is located at the membrane of the endoplasmic reticulum (17). Since it serves a physiologically important role in the glycogenolytic pathway, we hypothesized that glucose-6-phosphatase is required for BTIC survival, and that targeting it will commit BTICs to cell death.

In this work we report a regain of pro-malignant characteristics of BTICs following their recovery from glycolytic inhibition. We then identify that this recovery capacity is abolished

when the hepatic isoform of glucose-6-phosphatase (G6PC) is inhibited. Furthermore, knocking down G6PC is sufficient to decrease the migratory and proliferative capacity of BTICs. These findings seem to be related to the alterations in the glycogen metabolism of brain cancer cells.

Materials and Methods

Cell culture

All protocols in this study have been approved by the Johns Hopkins Hospital Institutional Review Board (IRB). Primary cultures of human fetal-derived astrocytes were obtained as described previously (18, 19). Adult glioblastoma tissue samples were collected after written informed consent. Patient characteristics are described in Table S1 (Table S1). Cell lines were tested and authenticated by the GRCF at Johns Hopkins. Control media consisted of DMEM F12 (+) glutamine (Life-technologies), BIT9500 10% (Stem Cell Technologies) for a final glucose concentration of 25 mM, and 20 ng/mL EGF and bFGF (Pepro Tech). 2DG-treated groups were cultured for 18hr in low glucose media consisting of DMEM no-glucose (+) glutamine, (Life-technologies) with BIT9500 (10%), 20 ng/mL EGF and bFGF (Pepro Tech) and 2-deoxyglucose (2-DG) 25 mM (Sigma-Aldrich). Recovery groups were obtained by replacing 2DG-supplemented media (after 18hr) with control media for 72hr. 0.1 mM chlorogenic acid (CHL) (Sigma-Aldrich) was added to recovery media in the recovery+CHL groups. CP-91149 40 μM (Selleckchem) was used as glycogen phosphorylase inhibitor when indicated. All treatments and experiments were carried out in a hypoxia incubator at an atmosphere of 5% carbon dioxide, 1.5% oxygen balanced with nitrogen, and 37°C.

Lentiviral transduction

Viruses were prepared in 293T cells. BTICs were transduced with equal titers of concentrated virus in control media supplemented with 1 μg/ml polybrene (Sigma) for 24hr and were given additional 24hr to recover before selection in 0.5 μg/ml puromycin (Sigma) for a minimum of 6 days.

Invasion assay

Boyden transwell assays were used to compare invasive capacity of BTICs among treatment groups. 5×10^4 cells in each treatment group were resuspended in corresponding media. 500 μl of cell suspension were seeded into the top well of a Boyden chamber (BD Biosciences; 8 μm pores); 700 μl of media were added to the lower chamber. After 24hr incubation at 37°C, cells were fixed, stained, and counted under light microscopy (10 fields per insert). All treatment groups were done in triplicate; all experiments were repeated three times.

Neurosphere assay

Neurosphere culture was performed as previously described by our group (20). Briefly, 2.5×10^3 BTICs were plated in uncoated T25 flasks in a total volume of 5 ml of control media. Size and number of spheres were measured after 14 days of culture and analyzed.

Migration assay

Migration of BTICs was assessed using topographic nanopatterned substratum which consists of parallel ridges 350 nm wide, 500 nm high, spaced 1.5 μm apart, fabricated onto glass coverslips as previously described by our group (21–23).

Tumor xenografts in nude mice

All animal protocols were approved by the Johns Hopkins Animal Care and Use Committee. 5×10^5 GBM1 BTICs were resuspended in 2 uL of media and injected intracranially into each of twenty-five male nude mice (Coordinates AP 1.34; ML 1.5; and DV 3.5) as previously described by our group (24).

Results

BTICs escape glycolytic inhibition with an aggressive phenotype

We performed all experiments using BTICs derived from intra-operative GBM samples. The capacity of our BTICs to form spheres in suspension, differentiate upon growth factor withdrawal, and form orthotopic tumors in animal models was previously described (Supplementary Fig. S1) (Table S1) (20, 25, 26). To recapitulate the hypoxic tumor niche, all the experiments were performed under chronic hypoxia.

First we evaluated the effects of the glycolytic inhibitor 2DG on primary BTICs and their recovery potential upon re-introduction of glucose to their media (Fig. 1A). We did this in effort to simulate the transitory exposure of the cells to the nutrient-restricted environment during cycles of intermittent tumor hypoxia *in vivo*. Targeting the glycolytic pathway by means of the glucose analogue 2DG has proven to sensitize cancer cells to additional treatments (27). However, specific cellular adaptations and functional consequences following glycolytic inhibition had not been recognized. To address this matter, we first evaluated BTIC proliferative capacity using 5-ethynyl-2-deoxyuridine (EdU) incorporation after 18hr exposure to 2DG. Compared to controls, 2DG-treated cells showed a decrease in proliferation ($p<0.001$). However, placing them back in control media for 72hr allowed them to recover from glycolytic inhibition (recovery group) ($p<0.001$) (Fig. 1B and Supplementary Fig. S2A).

We then evaluated the invasive capacity of BTICs using a transwell migration assay. As expected, glycolytic inhibition significantly impaired BTIC invasion (Fig. 1C). Interestingly, in the recovery group, the cells became more invasive when compared to the control and 2DG-treated groups ($p<0.001$) (Fig. 1C and Supplementary Fig. S2B–E). Next, we evaluated the expression of Matrix metalloproteinase-2 (MMP2) mRNA via qRT-PCR. MMP-2 is involved in the breakdown of extracellular matrix and is one of the proteins responsible for cancer cell metastasis (28). We observed a decrease in MMP-2 transcription levels in the 2DG-treated cells ($p<0.05$), while MMP2 mRNA levels significantly increased in the recovery group ($p<0.01$, compared to 2DG) (Fig. 1D and Supplementary Fig. S2F).

To evaluate the migratory cell speed, we used time-lapse microscopy images of cells migrating on a nanopatterned surface as previously described (22, 23). Addition of 2DG

significantly decreased the cell speed ($p<0.001$), while the recovery group cells showed an increase in their speed beyond that seen on both, control ($p<0.001$) and 2DG-treated groups ($p<0.001$) (Fig. 1E–H and Supplementary Movie S1).

2DG-treated BTICs demonstrated increased expression of p21 and p53 and decreased Cyclin D1. This alteration in expression of cell cycle proteins was accompanied by an increase in cell death, as evidenced by a rise in cleaved Poly ADP-ribose polymerase (PARP) expression. The reverse expression profile was seen in the recovery group (Fig. 1I and Supplementary Fig. S2G).

Lastly, we aimed to determine whether addition of 2DG affected the ability of BTICs to uptake glucose. We observed no significant changes after the addition of 2DG in three of our primary BTIC lines (GBM1, GBM2, and GBM3) (Supplementary Fig. S2H). Altogether, these results suggest that glycolytic inhibition induced by 2DG not only has a transient effect on BTICs, but more importantly, it stimulates their aggressiveness *in vitro*.

G6PC is up-regulated in BTICs

To investigate the mechanism underlying the recovery from 2DG, we evaluated potential enzymes that could be mediating this effect. During glycolysis, 2DG and glucose are both phosphorylated by hexokinase. Unlike glucose, the intermediate 2-deoxyglucose-6-phosphate (2DG-6P) cannot be further metabolized in the cell and accumulates, inhibiting glycolysis until it is de-phosphorylated (29). To determine if 2DG-6P dephosphorylation indeed mediated the recovery process, we examined the expression of several glucose phosphatases. We found that Glucose-6-phosphatase isoform α (G6PC) was up-regulated in human GBM samples. Through immunohistochemistry, we observed that G6PC had a stronger presence in the core and periphery of the tumor than in the non-cancer cortex (Fig. 2A–D). We then evaluated differential expression of G6PC between BTICs and non-cancer cortex cells from adult and fetal human brain via western blot and qRT-PCR. The expression of G6PC was higher in the GBM1 sample than in adult brain (AB) ($p<0.001$) or fetal samples (F1, F2, F3) ($p<0.05$, compared to F3) (Fig. 2E and Supplementary Fig. S3A). Next, we examined a panel of seven different primary derived BTICs. Each showed a consistent increase in G6PC when compared to the adult brain non-cancer cortex (Fig. 2F). The expression of G6PC has never been reported in brain cancer. To determine the exclusivity of the isoform's up-regulation, we also evaluated the expression of glucose 6-phosphatase isoform β (G6PC3), which had been reported to be expressed in the brain (30) but found no significant difference in its expression between normal adult brain, fetal brain, and BTICs (data not shown).

We next evaluated the effects of glycolytic inhibition via 2DG on the expression of G6PC in BTICs. Glycolytic inhibition induced an almost two-fold increase in expression of G6PC at both protein and mRNA levels ($p<0.01$) (Fig. 2G–H and Supplementary Fig. S3B–C). Culturing the cells in low glucose media for 18hr did not cause a significant change in the expression level of this isoform ($p=0.095$) (Supplementary Fig. S3B). However, in the recovery group a decrease in the expression of G6PC was observed ($p<0.01$) (Fig. 2G–H and Supplementary Fig. S3C and F). Collectively these results demonstrate that G6PC is more highly expressed in BTICs than in non-cancer cortex. The fact that the expression of

G6PC is further increased by 2DG suggests it has an important role in the recovery mechanism under investigation.

G6PC is required to recover (i.e. survive) from glycolytic inhibition

To further determine the involvement of G6PC in the recovery of BTICs from glycolytic inhibition, we performed a lentiviral-mediated knockdown of its gene (shG6PC) (Fig. 3A), and tested several key malignant cancer characteristics. The shG6PC in BTICs induced an increase in p21, p53 and cleaved PARP expression and a decrease in cyclin D1 (Fig. 3B). These effects were similar to those observed after induction of glycolytic inhibition with 2DG (Fig. 3B). We further investigated the protein level of two major transcription factors, hypoxia-inducible factor 1- α (HIF1α) and signal transducer and activator of transcription 3 (STAT3), known for causing enhancement in cancer cell survival, migration, and cellular metabolism (31, 32). We found that 2DG reduced the expression of these two proteins, however, recovered cells regained the expression of HIF1α and pSTAT3 (recovery group) (Fig. 3C). Down regulation of both HIF1α and pSTAT3 expression was also observed in the recovery-shG6PC group (Fig. 3C).

Additionally, we observed an increase in the activation of caspase-3 ($p<0.001$) and a decrease in cell proliferation ($p<0.001$) in the control-shG6PC cells when compared to the control-EV cells (Fig. 3D and E and Supplementary Fig. S3D). Next, we investigated two of the most critical malignant properties of glioblastoma, invasion and migration. shG6PC strongly decreased the cell's ability to invade ($p<0.001$) and migrate ($p<0.001$) when compared to EV cells (Fig. 3F–G and Supplementary Fig. S3E, S4 and Movie S2).

To evaluate if the effects observed after knocking-down G6PC could be mimicked chemically, we tested the effects of chlorogenic acid (CHL), an inhibitor of glucose-6-phosphate translocase, which transports glucose-6-phosphate from the cytoplasm into the lumen of the endoplasmic reticulum (33). At the transcription level, we found that recovery of CHL-treated BTICs displayed increased transcription levels of G6PC when compared to those of the control ($p<0.01$), suggesting a rescue mechanism induced in recovery group to CHL (Supplementary Fig. 3F). Interestingly, recovered CHL-treated cells displayed a significant reduction in cell invasion when compared to non-treated recovered cells ($p<0.05$) (Fig. 3H). CHL treatment also decreased cell migration in recovered cells ($p<0.05$) (Fig. 3I and Supplementary Fig. S3G). To determine if these findings were specific to BTICs, we evaluated the invasive capacity of other human cancer cell lines, upon G6PC-Knockdown. We tested human breast adenocarcinoma (MDA-MB-231), human melanoma (A375), and human pancreatic carcinoma (Panc-1) cell lines. While the effects of shG6PC were similar in the pancreatic cells (a decrease in their invasive capacity), this result was not observed in the cells of breast or melanoma origin when compared to brain tumors (Supplementary Fig. S3H). Collectively, these results demonstrate that not only does shG6PC prevent escape from glycolytic inhibition in BTICs, but also induces a decrease in migration, invasion and cell viability *in vitro*.

G6PC regulates astrocytic differentiation in BTICs

We previously observed that glycolytic inhibition induced the commitment of glioma cells to a neuronal lineage (16). Building upon this work, we were interested in evaluating the morphology and expression of differentiation markers in our experimental groups. Expression of the progenitor cell marker nestin, the astrocytic marker GFAP and the neuronal marker Tuj1 were examined before and after 2DG exposure. In GBM1 we found a significant decrease in the number of nestin-positive cells in the 2DG group ($p<0.05$) (Supplementary Fig. S5A–B). Consistent with our previous results (16), we observed no significant increase in the GFAP-expressing cells ($p=0.8248$) (Supplementary Fig. S5A and S5C), however, 2DG did induce an increase in Tuj1 compared to controls ($p<0.05$) (Supplementary Fig. S5A and S5D). These results suggest that glycolytic inhibition with 2DG induces differentiation towards a neuronal lineage, shown as an increase in Tuj1.

Microscopic observation of BTICs after shG6PC revealed major alterations in their morphology. Unlike the flat polygonal morphology of the control cells, the shape of shG6PC cells was similar to that of mature astrocytes (Fig. 4A). To further explore this finding, we examined the expression of Tuj1 and GFAP after shG6PC. Immunocytochemical staining confirmed a significant decrease in the expression of Tuj1 after shG6PC in both control and recovery groups ($p<0.001$). However, a concomitant up-regulation of GFAP expression was observed in the control-shG6PC group ($p<0.001$) and was higher in the recovery group ($p<0.01$) (Fig. 4B–C). These findings were consistent with the results obtained after the addition of CHL (Supplementary Fig. S5). No significant changes were observed in nestin expression after knocking down G6PC or adding CHL (data not shown). Altogether these findings indicate that shG6PC can induce differentiation of BTICs into an astrocytic lineage. This led us to further investigate the possible role that G6PC might play on the stem-like properties of BTICs. This subpopulation of tumor cells is believed to play a major role in tumor recurrence (34).

G6PC is required for maintenance of stem-like properties in BTICs

Neurosphere formation assays are currently the standard *in vitro* method for identifying the presence of stem cells derived from both tumor and non-tumor tissues (35–37). Therefore, we determined the role of G6PC in a sphere formation assay. Two weeks post lentiviral transduction we evaluated the sphere forming capacity of control, 2DG, and recovery groups. shG6PC significantly decreased sphere formation ($p<0.001$) and size (control $p<0.01$, recovery $p<0.001$) in both control and recovery groups (Fig. 4D–F). Next, we sought to investigate the expression of CD133, a membrane marker used to enrich for stem cells and expressed by both neural stem cells and brain cancer stem cells (38, 39). We found that the addition of 2DG strongly decreased the expression of CD133 in control-EV cells (data not shown). Furthermore, culturing of the EV 2DG cells in control media for 72 hr (recovery) allowed them to rescue (or induce) expression of CD133 (Fig. 4G). However, shG6PC dramatically decreased the expression of CD133 in both control and recovery cells ($p<0.05$) (Fig. 4G).

Lastly, we evaluated the expression of Akt, a well-characterized downstream key effector of the phospoinositide 3-kinase (PI3K), since Akt is commonly up-regulated in human cancers

(40) and is known to play an important role in the regulation of proliferation and cell survival (41). Moreover, it has been suggested that CD133 plays an important role in the activation of the Akt pathway in glioma stem cells (42). We thus investigated whether the decrease in CD133, after shG6PC, was associated with a decrease in the activation of Akt. Through immunoblot analysis, we found that there was indeed a significant decrease in pAkt (Ser473) in both control and recovery groups after shG6PC (Fig. 4H). Together, our results suggest that G6PC is required for sphere formation and plays a positive role in the activation of the cytoprotective Akt pathway – possibly through CD133.

G6PC knockdown promotes glycogen accumulation

Recent studies have suggested the critical role of glycogen in promoting cancer cell survival (43, 44). Moreover, inhibiting glycogen breakdown induces apoptosis and early cell senescence in cancer cells (43, 44). Given the physiological importance of G6PC in the glycogenolytic pathway, we proceeded to investigate glycogen metabolism after shG6PC.

Glucose-6-phosphate is an allosteric activator of glycogen synthase which regulates glycogen synthesis (45, 46). We hypothesized that shG6PC would lead to glycogen over-accumulation and decrease the malignant phenotype of our BTICs. To test this hypothesis, first we examined the intracellular glycogen levels of our groups. We found that shG6PC promoted glycogen accumulation in all groups (Fig. 5A). We then examined the expression of glycogen synthase (GS) and glycogen phosphorylase (GP) key enzymes that regulate synthesis and degradation of glycogen, respectively (47, 48). Previous studies have found that hypoxia induced an increase in the expression of the muscle isoform of glycogen synthase (GYS1), and the liver isoform of glycogen phosphorylase (PYGL) in glioblastoma cells (43). Therefore, we decided to investigate the expression of these two isoforms in our BTICs.

At the protein level, there was a decrease in inactive, phosphorylated GYS1 (serine 641) in all groups after shG6PC when compared to the EV groups (Fig. 5B and Supplementary Fig. S6A). GYS1 mRNA was found to be significantly higher in shG6PC-control group when compared to the EV-control group ($p<0.001$) (Supplementary Fig. S6C). These results were in accordance with the increase in GYS1 activity (Supplementary Fig. S6A). Moreover, in shG6PC groups, the PYGL protein level was found to be significantly decreased when compared to the EV groups (Fig. 5B and Supplementary Fig. S6B). However, at the mRNA level PYGL was found to be decreased only in the 2DG and recovery shG6PC groups ($p<0.01$) (Supplementary Fig. S6D). These findings imply that shG6PC cells exhibit an uncontrolled increase in glycogen synthesis while EVs exhibit a preference for glycogen degradation.

Prior to its entry into the glycolytic or pentose phosphate pathways, glycogen is converted to glucose-1-phosphate by glycogen phosphorylase (GP) (49). Utilizing the GP inhibitor CP-91149 (GPi), we determined the consequences of preventing the conversion of glycogen to glucose-1-phosphate on cell invasion and proliferation (Fig. 5C). The presence of GPi decreased the ability of BTICs to invade in control, 2DG, and recovery EV groups ($p<0.001$) (Fig. 5D–G), indicating that the conversion of endogenous glycogen to glucose-1-phosphate plays a critical role in GBM cell invasion. Strikingly, the addition of GPi to shG6PC cells,

further decreased cell invasion in all conditions (control $p<0.001$, 2DG $p<0.05$, recovery $p<0.001$) (Fig. 5D–G). Next, we sought to investigate the effect of GPi on cell proliferation. In EV cells, GP inhibition induced a decrease in cell proliferation in both control and recovery groups (control $p<0.001$, recovery $p<0.01$) (Fig. 5H and J). In shG6PC cells there was a decrease in cell proliferation exclusively in the recovery group (data not shown). These data support the hypothesis that G6PC is required for cells to fully eliminate 2DG and recover their proliferative capacity. Incubation of cells with GPi and 2DG did not demonstrate any additional effect on cell proliferation (Fig. 5I), presumably due to the profound cell proliferation inhibition obtained with 2DG.

Uncontrolled glycogen accumulation has been shown to lead to cell death and to have deleterious consequences in cancer cells. These results provide a potential mechanism accounting for the phenotype observed in the shG6PC cells, i.e. through an accumulation of glycogen.

G6PC mediates invasiveness of brain cancer *in vivo*

To test the *in vivo* roles of G6PC during cancer development, GBM1 with shG6PC or EV were implanted intracranially into athymic nude mice, as described previously (Fig. 6A) (23, 24). We evaluated the proliferation and invasive capacity of BTICs through the corpus callosum seven weeks after transplantation (Supplementary Fig. S7A). Ki67 staining was performed to evaluate the proliferation index. We found that the total number of Ki67 positive cells was significantly lower after knocking down G6PC in both control and recovery ($p<0.001$) (Fig. 6B, and Supplementary Fig. S7B). However, after determining proliferation index, we found no significant difference between groups (Supplementary Fig. S7C). This may be due to the increase in cell death as demonstrated by the *in vitro* activation of caspase-3 after shG6PC (Fig. 3D). More importantly, cell counts across the corpus callosum revealed that shG6PC resulted in a profound reduction in the invasiveness of BTICs in both control and recovery groups ($p<0.001$) (Fig. 6C–E and Supplementary Fig. S7D). These findings strongly suggest that G6PC could be playing an important role *in vivo* in regulating cell invasion, one of the biggest determinants in the recurrence and progression of GBM.

Discussion

Our results are the first to demonstrate a relationship between G6PC, glycolytic inhibition and BTICs aggressiveness via glycogen metabolism. In this study, we provide evidence that BTICs are able to find alternative survival pathways to escape glycolytic inhibition and acquire a more aggressive phenotype in doing so. We further propose that the ability of BTICs to counteract glycolytic inhibition occurs, at least partly, via a G6PC dependent mechanism potentially through intracellular glycogen degradation. Our hypothesis is supported by the observation that shG6PC prevented the recovery from glycolytic inhibition and resulted in a decreased aggressive phenotype and increased glycogen accumulation.

We observed that BTICs recovered from glycolytic inhibition and were more invasive, migratory, and proliferative compared to control cells. We believe that this increase in invasion, migration, and proliferation is analogous to the cellular responses that occur during

the cyclic hypoxia phenomenon in which growth of the tumor increases once it recovers from hypoxia/nutrient deprivation and is consistent with previous studies that also reported an increase in tumorigenesis and selection for cancer initiating cells following hypoxia and or nutrient deprivation (14, 50).

We utilized 2DG as a model of glycolytic inhibition. 2DG is a glucose analogue that is phosphorylated by hexokinase to inhibit glycolysis (51). Knowing that a phosphatase was required to clear the cell from its presence (29), we tested the expression of glucose 6 phosphatase isoform α (G6PC) and the ubiquitously expressed glucose 6 phosphatase isoform β (G6PC3). We found up-regulation of G6PC and no significant increase of G6PC3 after the addition of 2DG.

G6PC is a phosphatase that is predominantly expressed in the liver, kidney, and β-cells of the pancreatic islets (17). No studies have looked specifically at the expression of G6PC in BTICs. We tested the expression of G6PC in several primary derived glioma BTICs and on tissue samples and found it to be highly up-regulated.

We found that BTICs utilize G6PC to counteract glycolytic inhibition and depend on it even in the absence of glycolytic inhibition. Evidence for this was first suggested by the up-regulation of G6PC expression upon 2DG treatment and further corroborated by the observation that inhibiting G6PC in BTICs stops their ability to recover from glycolytic inhibition. Remarkably the sole knockdown of G6PC was able to decrease the aggressive phenotype of BTICs potentially through the down-regulation of the CD133/AKT axis and an increase in glycogen accumulation which has been previously shown to induce cell death in cancer cells if it is not properly metabolized (43, 44). Glycogen was recently identified as a marker of astrocytic differentiation (52). Interestingly, we also observed astrocytic differentiation along with glycogen accumulation in the shG6PC BTICs.

Collectively, these results demonstrate that not only does G6PC-knockdown prevent the escape from glycolytic inhibition in BTICs, but it also induces a decrease in migration, invasion and cell viability; a phenomenon that is worth exploring in other cancers.

In the liver, targeted deletion of G6PC induces glucose-6-phosphate and glycogen accumulation (53). A number of observations have suggested that cancer cells have increased levels of glycogen (54), and that hypoxia stimulates glycogen buildup for later use in several cancer cell lines (13). Furthermore, in U87 glioma cells, glycogen accumulation induces premature cell senescence (43). Therefore, it is possible that altered glycogen metabolism could be part of the survival mechanism adopted by BTICs upon glycolytic inhibition, and thus a potential therapeutic target.

We observed in our BTICs that shG6PC induces an increase in the activity of GYS1, a decrease in PYGL, and subsequent glycogen accumulation. Given that accumulation of glucose-6-phosphate activates GYS1 and inhibits PYGL (45, 46), we hypothesized that glycogen levels increased upon shG6PC possibly as a result of glucose-6-phosphate accumulation (Fig. 7). This suggests that the channeling of glucose through glycogen may possess additional physiological functions that go beyond its role as an energy source in situations with increased glucose demand. Furthermore, we found that HIF1α and STAT3 to

be significantly down regulated upon shG6PC. Interestingly, HIF1α and STAT3 are found to be, at least in part, involved in glycogen regulation (13, 55). For instance, the expression of the G6PC is also regulated by HIF1α in hepatocytes (56). The specific role of HIF1α and STAT3 in the response of BTICs to G6PC inhibition need to be further investigated.

In summary, this work gives a novel insight on the expression and effects of G6PC in primary BTICs and contributes to our understanding of the metabolic adaptations occurring in cancer cells. The heightened expression of G6PC in GBMs when compared to normal brain can potentially serve as a novel therapeutic target that could render brain cancer cells less aggressive and more vulnerable to additional metabolic inhibitors.

Supplementary Material

Refer to Web version on PubMed Central for supplementary material.

Acknowledgments

Grant Support: This project was supported by NIH R01 NS070024 (A. Quinones-Hinojosa), MSCRF (H. Guerrero-Cazares), and HHMI (A. Quinones-Hinojosa and A. Abutaleb).

We thank Lakesha Johnson and Liron Noiman for establishing primary cell cultures of these primary GBM specimens; Colette ap Rhys for her help with the viral work; and Otavia L. Caballero, for helping with IHC staining for G6PC.

References

1. Stupp R, Hegi ME, Mason WP, van den Bent MJ, Taphoorn MJ, Janzer RC, et al. Effects of radiotherapy with concomitant and adjuvant temozolomide versus radiotherapy alone on survival in glioblastoma in a randomised phase III study: 5-year analysis of the EORTC-NCIC trial. The lancet oncology. 2009; 10:459–66. [PubMed: 19269895]
2. Chaichana KL, Zadnik P, Weingart JD, Olivi A, Gallia GL, Blakeley J, et al. Multiple resections for patients with glioblastoma: prolonging survival. Journal of neurosurgery. 2013; 118:812–20. [PubMed: 23082884]
3. Walbert T, Mikkelsen T. Recurrent high-grade glioma: a diagnostic and therapeutic challenge. Expert review of neurotherapeutics. 2011; 11:509–18. [PubMed: 21469924]
4. Hanahan D, Weinberg RA. Hallmarks of cancer: the next generation. Cell. 2011; 144:646–74. [PubMed: 21376230]
5. Galli R, Binda E, Orfanelli U, Cipelletti B, Gritti A, De Vitis S, et al. Isolation and characterization of tumorigenic, stem-like neural precursors from human glioblastoma. Cancer research. 2004; 64:7011–21. [PubMed: 15466194]
6. Venere M, Fine HA, Dirks PB, Rich JN. Cancer stem cells in gliomas: identifying and understanding the apex cell in cancer's hierarchy. Glia. 2011; 59:1148–54. [PubMed: 21547954]
7. Dewhirst MW. Relationships between cycling hypoxia, HIF-1, angiogenesis and oxidative stress. Radiat Res. 2009; 172:653–65. [PubMed: 19929412]
8. Cairns RA, Kalliomaki T, Hill RP. Acute (cyclic) hypoxia enhances spontaneous metastasis of KHT murine tumors. Cancer Res. 2001; 61:8903–8. [PubMed: 11751415]
9. Carmeliet P, Jain RK. Molecular mechanisms and clinical applications of angiogenesis. Nature. 2011; 473:298–307. [PubMed: 21593862]
10. Soda Y, Myskiw C, Rommel A, Verma IM. Mechanisms of neovascularization and resistance to anti-angiogenic therapies in glioblastoma multiforme. J Mol Med (Berl). 2013; 91:439–48. [PubMed: 23512266]
11. Mohyeldin A, Garzon-Muvdi T, Quinones-Hinojosa A. Oxygen in stem cell biology: a critical component of the stem cell niche. Cell stem cell. 2010; 7:150–61. [PubMed: 20682444]

12. Warburg O. On the origin of cancer cells. Science. 1956; 123:309–14. [PubMed: 13298683]
13. Pelletier J, Bellot G, Gounon P, Lacas-Gervais S, Pouyssegur J, Mazure NM. Glycogen Synthesis is Induced in Hypoxia by the Hypoxia-Inducible Factor and Promotes Cancer Cell Survival. Front Oncol. 2012; 2:18. [PubMed: 22649778]
14. Flavahan WA, Wu Q, Hitomi M, Rahim N, Kim Y, Sloan AE, et al. Brain tumor initiating cells adapt to restricted nutrition through preferential glucose uptake. Nature neuroscience. 2013
15. Wolf A, Agnihotri S, Guha A. Targeting metabolic remodeling in glioblastoma multiforme. Oncotarget. 2010; 1:552–62. [PubMed: 21317451]
16. Pistollato F, Abbadi S, Rampazzo E, Viola G, Della Puppa A, Cavallini L, et al. Hypoxia and succinate antagonize 2-deoxyglucose effects on glioblastoma. Biochemical pharmacology. 2010; 80:1517–27. [PubMed: 20705058]
17. Lei KJ, Shelly LL, Pan CJ, Sidbury JB, Chou JY. Mutations in the glucose-6-phosphatase gene that cause glycogen storage disease type 1a. Science. 1993; 262:580–3. [PubMed: 8211187]
18. Ravin R, Blank PS, Steinkamp A, Rappaport SM, Ravin N, Bezrukov L, et al. Shear forces during blast, not abrupt changes in pressure alone, generate calcium activity in human brain cells. PLoS One. 2012; 7:e39421. [PubMed: 22768078]
19. Tzeng SY, Guerrero-Cazares H, Martinez EE, Sunshine JC, Quinones-Hinojosa A, Green JJ. Non-viral gene delivery nanoparticles based on poly(beta-amino esters) for treatment of glioblastoma. Biomaterials. 2011; 32:5402–10. [PubMed: 21536325]
20. Guerrero-Cazares H, Chaichana KL, Quinones-Hinojosa A. Neurosphere culture and human organotypic model to evaluate brain tumor stem cells. Methods Mol Biol. 2009; 568:73–83. [PubMed: 19582422]
21. Kim DH, Han K, Gupta K, Kwon KW, Suh KY, Levchenko A. Mechanosensitivity of fibroblast cell shape and movement to anisotropic substratum topography gradients. Biomaterials. 2009; 30:5433–44. [PubMed: 19595452]
22. Kim DH, Seo CH, Han K, Kwon KW, Levchenko A, Suh KY. Guided Cell Migration on Microtextured Substrates with Variable Local Density and Anisotropy. Advanced functional materials. 2009; 19:1579–86. [PubMed: 20046799]
23. Garzon-Muvdi T, Schiapparelli P, ap Rhys C, Guerrero-Cazares H, Smith C, Kim DH, et al. Regulation of brain tumor dispersal by NKCC1 through a novel role in focal adhesion regulation. PLoS biology. 2012; 10:e1001320. [PubMed: 22570591]
24. Gonzalez-Perez O, Guerrero-Cazares H, Quinones-Hinojosa A. Targeting of deep brain structures with microinjections for delivery of drugs, viral vectors, or cell transplants. Journal of visualized experiments : JoVE. 2010
25. Li Y, Li A, Glas M, Lal B, Ying M, Sang Y, et al. c-Met signaling induces a reprogramming network and supports the glioblastoma stem-like phenotype. Proceedings of the National Academy of Sciences of the United States of America. 2011; 108:9951–6. [PubMed: 21628563]
26. Ying M, Sang Y, Li Y, Guerrero-Cazares H, Quinones-Hinojosa A, Vescovi AL, et al. Kruppel-like family of transcription factor 9, a differentiation-associated transcription factor, suppresses Notch1 signaling and inhibits glioblastoma-initiating stem cells. Stem Cells. 2011; 29:20–31. [PubMed: 21280156]
27. Cheng G, Zielonka J, Dranka BP, McAllister D, Mackinnon AC Jr, Joseph J, et al. Mitochondria-targeted drugs synergize with 2-deoxyglucose to trigger breast cancer cell death. Cancer Res. 2012; 72:2634–44. [PubMed: 22431711]
28. Guo P, Imanishi Y, Cackowski FC, Jarzynka MJ, Tao HQ, Nishikawa R, et al. Up-regulation of angiopoietin-2, matrix metalloprotease-2, membrane type 1 metalloprotease, and laminin 5 gamma 2 correlates with the invasiveness of human glioma. The American journal of pathology. 2005; 166:877–90. [PubMed: 15743799]
29. Nelson CA, Wang JQ, Leav I, Crane PD. The interaction among glucose transport, hexokinase, and glucose-6-phosphatase with respect to 3H-2-deoxyglucose retention in murine tumor models. Nuclear medicine and biology. 1996; 23:533–41. [PubMed: 8832712]
30. Ghosh A, Cheung YY, Mansfield BC, Chou JY. Brain contains a functional glucose-6-phosphatase complex capable of endogenous glucose production. The Journal of biological chemistry. 2005; 280:11114–9. [PubMed: 15661744]

31. Semenza GL. Targeting HIF-1 for cancer therapy. Nature reviews Cancer. 2003; 3:721–32.
32. Yu H, Jove R. The STATs of cancer--new molecular targets come of age. Nature reviews Cancer. 2004; 4:97–105.
33. van Dijk TH, van der Sluijs FH, Wiegman CH, Baller JF, Gustafson LA, Burger HJ, et al. Acute inhibition of hepatic glucose-6-phosphatase does not affect gluconeogenesis but directs gluconeogenic flux toward glycogen in fasted rats. A pharmacological study with the chlorogenic acid derivative S4048. The Journal of biological chemistry. 2001; 276:25727–35. [PubMed: 11346646]
34. Dirks PB. Brain tumour stem cells: the undercurrents of human brain cancer and their relationship to neural stem cells. Philosophical transactions of the Royal Society of London Series B, Biological sciences. 2008; 363:139–52.
35. Chaichana K, Zamora-Berridi G, Camara-Quintana J, Quinones-Hinojosa A. Neurosphere assays: growth factors and hormone differences in tumor and nontumor studies. Stem Cells. 2006; 24:2851–7. [PubMed: 16945995]
36. Chaichana KL, Guerrero-Cazares H, Capilla-Gonzalez V, Zamora-Berridi G, Achanta P, Gonzalez-Perez O, et al. Intra-operatively obtained human tissue: protocols and techniques for the study of neural stem cells. Journal of neuroscience methods. 2009; 180:116–25. [PubMed: 19427538]
37. Vescovi AL, Galli R, Reynolds BA. Brain tumour stem cells. Nature reviews Cancer. 2006; 6:425–36.
38. Singh SK, Clarke ID, Terasaki M, Bonn VE, Hawkins C, Squire J, et al. Identification of a cancer stem cell in human brain tumors. Cancer research. 2003; 63:5821–8. [PubMed: 14522905]
39. Bao S, Wu Q, McLendon RE, Hao Y, Shi Q, Hjelmeland AB, et al. Glioma stem cells promote radioresistance by preferential activation of the DNA damage response. Nature. 2006; 444:756–60. [PubMed: 17051156]
40. LoPiccolo J, Blumenthal GM, Bernstein WB, Dennis PA. Targeting the PI3K/Akt/mTOR pathway: effective combinations and clinical considerations. Drug resistance updates : reviews and commentaries in antimicrobial and anticancer chemotherapy. 2008; 11:32–50. [PubMed: 18166498]
41. Datta SR, Dudek H, Tao X, Masters S, Fu H, Gotoh Y, et al. Akt phosphorylation of BAD couples survival signals to the cell-intrinsic death machinery. Cell. 1997; 91:231–41. [PubMed: 9346240]
42. Wei Y, Jiang Y, Zou F, Liu Y, Wang S, Xu N, et al. Activation of PI3K/Akt pathway by CD133-p85 interaction promotes tumorigenic capacity of glioma stem cells. Proceedings of the National Academy of Sciences of the United States of America. 2013; 110:6829–34. [PubMed: 23569237]
43. Favaro E, Bensaad K, Chong MG, Tennant DA, Ferguson DJ, Snell C, et al. Glucose utilization via glycogen phosphorylase sustains proliferation and prevents premature senescence in cancer cells. Cell metabolism. 2012; 16:751–64. [PubMed: 23177934]
44. Lee WN, Guo P, Lim S, Bassilian S, Lee ST, Boren J, et al. Metabolic sensitivity of pancreatic tumour cell apoptosis to glycogen phosphorylase inhibitor treatment. Br J Cancer. 2004; 91:2094–100. [PubMed: 15599384]
45. Bouskila M, Hunter RW, Ibrahim AF, Delattre L, Peggie M, van Diepen JA, et al. Allosteric regulation of glycogen synthase controls glycogen synthesis in muscle. Cell metabolism. 2010; 12:456–66. [PubMed: 21035757]
46. Aiston S, Andersen B, Agius L. Glucose 6-phosphate regulates hepatic glycogenolysis through inactivation of phosphorylase. Diabetes. 2003; 52:1333–9. [PubMed: 12765941]
47. Roach PJ, Cheng C, Huang D, Lin A, Mu J, Skurat AV, et al. Novel aspects of the regulation of glycogen storage. Journal of basic and clinical physiology and pharmacology. 1998; 9:139–51. [PubMed: 10212831]
48. Newgard CB, Hwang PK, Fletterick RJ. The family of glycogen phosphorylases: structure and function. Critical reviews in biochemistry and molecular biology. 1989; 24:69–99. [PubMed: 2667896]
49. Moller DE. New drug targets for type 2 diabetes and the metabolic syndrome. Nature. 2001; 414:821–7. [PubMed: 11742415]

50. Osawa T, Muramatsu M, Watanabe M, Shibuya M. Hypoxia and low-nutrition double stress induces aggressiveness in a murine model of melanoma. Cancer science. 2009; 100:844–51. [PubMed: 19220297]
51. Beneteau M, Zunino B, Jacquin MA, Meynet O, Chiche J, Pradelli LA, et al. Combination of glycolysis inhibition with chemotherapy results in an antitumor immune response. Proc Natl Acad Sci U S A. 2012; 109:20071–6. [PubMed: 23169636]
52. Brunet JF, Allaman I, Magistretti PJ, Pellerin L. Glycogen metabolism as a marker of astrocyte differentiation. Journal of cerebral blood flow and metabolism : official journal of the International Society of Cerebral Blood Flow and Metabolism. 2010; 30:51–5.
53. Mutel E, Abdul-Wahed A, Ramamonjisoa N, Stefanutti A, Houberdon I, Cavassila S, et al. Targeted deletion of liver glucose-6 phosphatase mimics glycogen storage disease type 1a including development of multiple adenomas. J Hepatol. 2011; 54:529–37. [PubMed: 21109326]
54. Rousset M, Zweibaum A, Fogh J. Presence of glycogen and growth-related variations in 58 cultured human tumor cell lines of various tissue origins. Cancer Res. 1981; 41:1165–70. [PubMed: 7459858]
55. Moh A, Zhang W, Yu S, Wang J, Xu X, Li J, et al. STAT3 sensitizes insulin signaling by negatively regulating glycogen synthase kinase-3 beta. Diabetes. 2008; 57:1227–35. [PubMed: 18268048]
56. Gautier-Stein A, Soty M, Chilloux J, Zitoun C, Rajas F, Mithieux G. Glucotoxicity induces glucose-6-phosphatase catalytic unit expression by acting on the interaction of HIF-1alpha with CREB-binding protein. Diabetes. 2012; 61:2451–60. [PubMed: 22787137]

Implications

This study is the first to demonstrate a functional relationship between the critical gluconeogenic and glycogenolytic enzyme G6PC with the metabolic adaptations during GBM invasion.

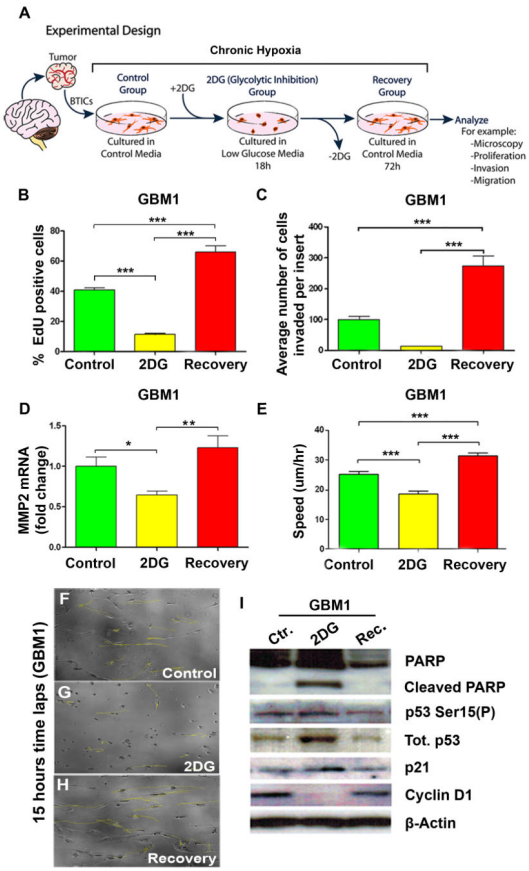

Figure 1. Brain tumor initiating cells (BTICs) recover from glycolytic inhibition with a more aggressive phenotype

(A) Schematization of the experimental design. Control cells were cultured in control media. 2DG (25 mM) was added to low glucose media for 18hr (2DG group) to inhibit glycolysis and removed to allow cells to recover for 72hr in control media (recovery group). (B) Mean proliferation using EdU incorporation via flow cytometry. (C) Comparison of the invasive capacity of BTICs using a Transwell Boyden chamber. (D) MMP2 mRNA expression in BTICs. (E) Instantaneous migration speed of BTICs quantified as a function of time (n≥60 cells). (F–H) Representative moving trajectories of individual BTICs (colored in yellow) in a nanopatterned surface during a 15h time-lapse microscopy. (I) Representative western blot for PARP, cleaved PARP, phosphorylated p53 (Ser 15), p53, p21 and Cyclin D1. The data are presented as the mean ± S.E.M (n=3) from three independent experiments using GBM1. (*: $p<0.05$, **: $p<0.01$, ***: $p<0.001$).

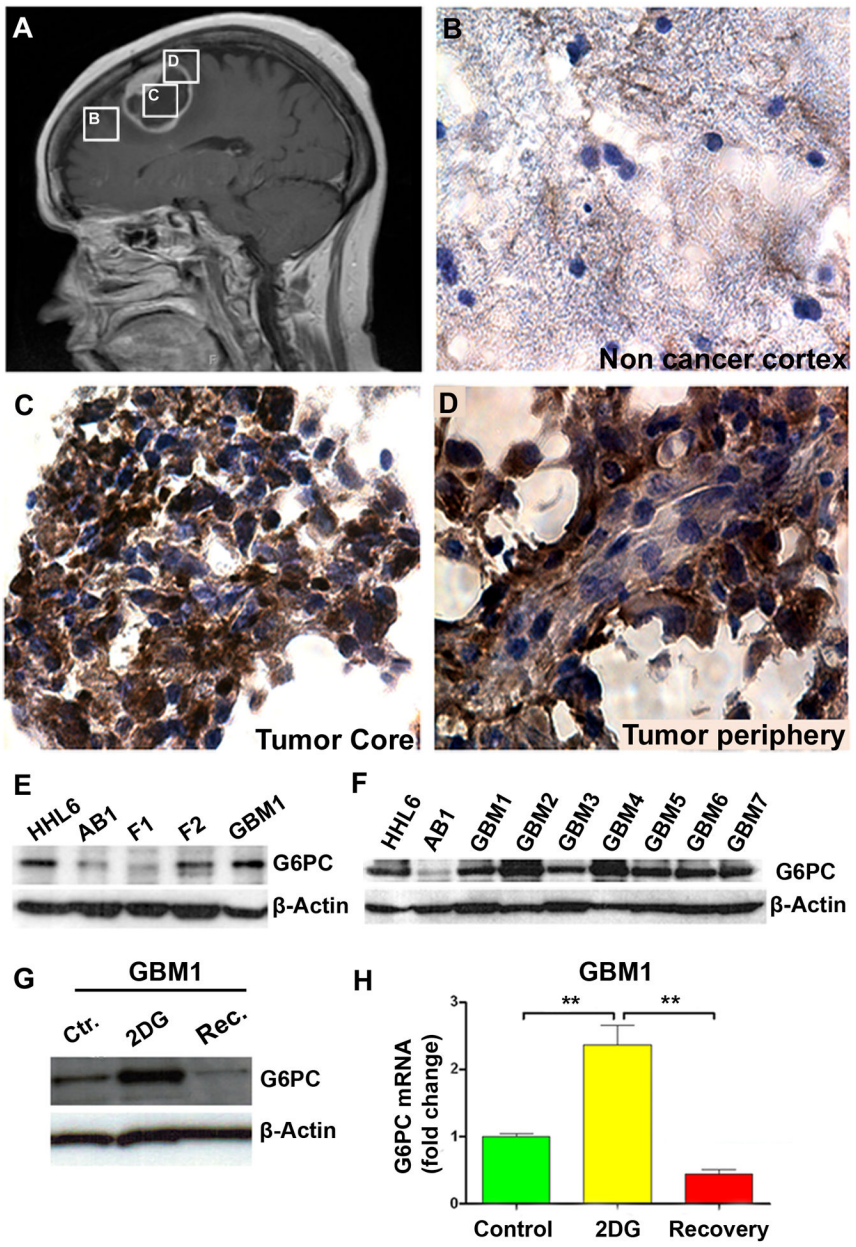

Figure 2. G6PC is up-regulated in glioblastomas compared to fetal brain and adult non-cancerous human cortex

(A) Post-contrast sagittal T1 weighted MRI demonstrating a centrally necrotic, peripherally enhancing mass in the right frontal lobe (GBM8). Boxes represent areas from which tissue samples were obtained. (B–D) Immunohistochemistry staining for G6PC performed on non-cancerous cortex (B), tumor core tissue (C) and tumor peripheral tissue (D) from the same patient (GBM8). (E–F) Immunoblot analyses for G6PC in two different fetal-derived cells (F1 and F2) and in 7 different BTICs (GBM1-GBM7). Hepatocytes were used as positive controls (HHL6), and non-cancerous cortex from adult brain (AB1) as negative controls. (G–H) G6PC protein and mRNA measurements in GBM1. The data are presented as the mean ± S.E.M (n=3) from three independent experiments. (**: $p<0.01$).

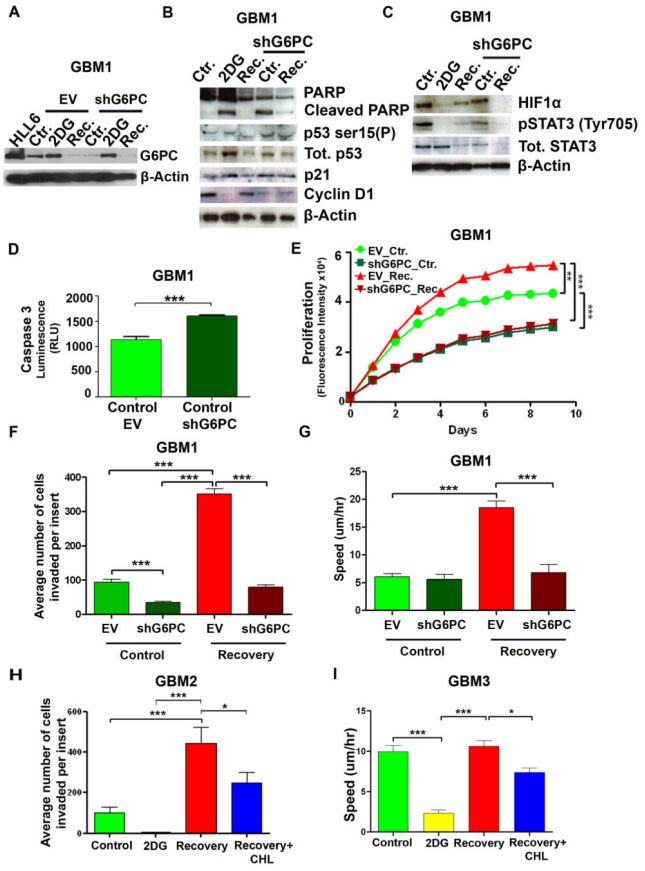

Figure 3. shG6PC decreases cell viability, invasion, and migration in BTICs

(A) Representative immunoblot for G6PC in EV (empty vector) and shG6PC GBM1. (B–C) Immunoblots for PARP, cleaved PARP, phosphorylated p53(Ser 15), p53, p21, Cyclin D1, HIF1α, total STAT3 and pSTAT3 in EV or shG6PC transduced GBM1. (D) Caspase 3/7 activity assay comparing control-EV and control-shG6PC GBM1. (E) Cell viability and proliferation were evaluated using alamarBlue in GBM1 EV or shG6PC. (F) Comparison of the invasive capacity of GBM1 using a Transwell Boyden chamber. (G) Instantaneous migration speed of GBM1 quantified as a function of time (n≥60 cells). (H) Comparison of the invasive capacity of GBM2. (I) Instantaneous migration speed of GBM3 quantified as a function of time (n≥60 cells). In H–I, recovering cells (recovery+CHL groups) were treated with chlorogenic acid (CHL 100μM) for 72hr to inhibit G6PC. The data are presented as the mean ± S.E.M (n=3) from three independent experiments (*: p<0.05, ***: p<0.001).

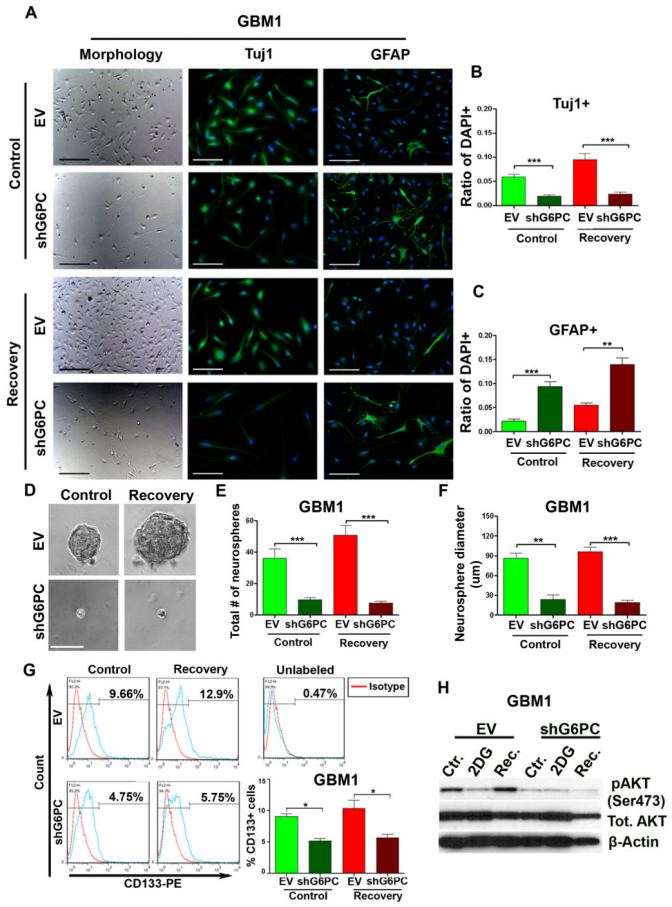

Figure 4. shG6PC of BTICs induces astrocytic differentiation and decreases stemness

(A–C) Immunocytochemistry staining comparing the expression of Tuj1 and GFAP in GBM1. (D–F) Neurosphere assay comparing sphere size and number in GBM1. (G) Flow cytometric analysis of the expression of CD133 in GBM1. (H) Representative western blot of total and pAKT(Ser473) in GBM1. The data are presented as the mean ± S.E.M (n=3) from three independent experiments. (*: $p<0.05$, **: $p<0.01$, ***: $p<0.001$). Scale bars=100 μm.

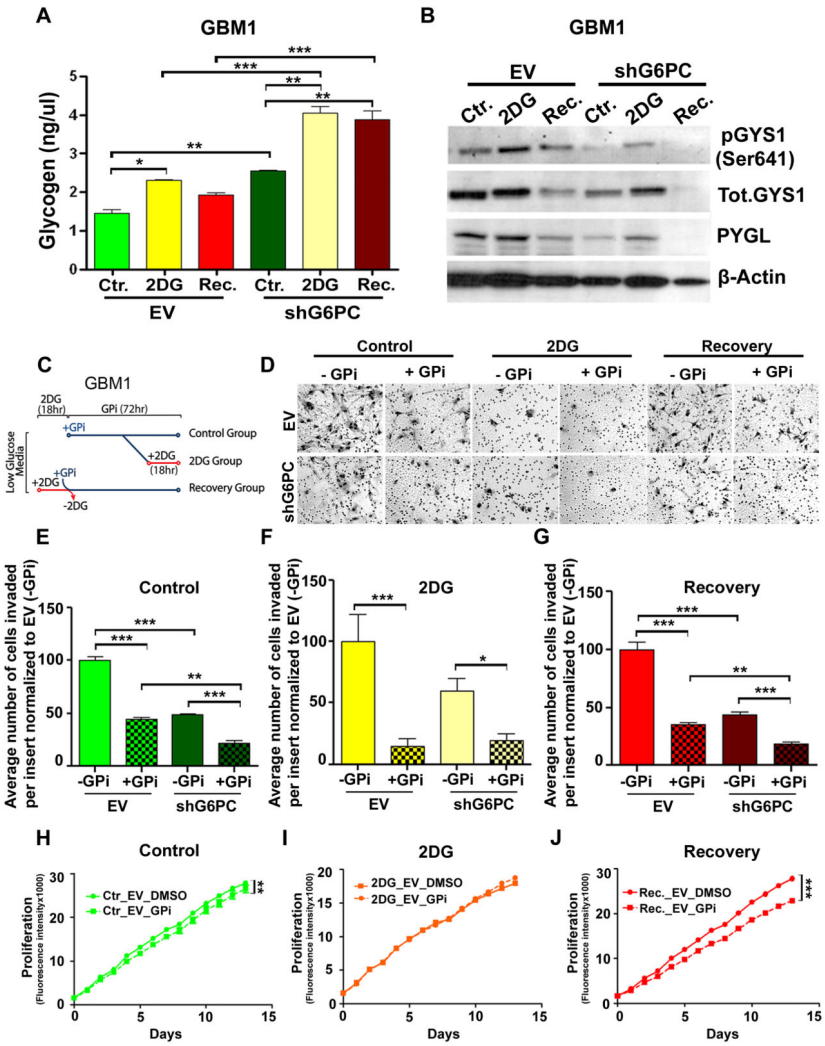

Figure 5. shG6PC induces glycogen accumulation through activation of Glycogen synthase (GYS1) and inhibition of Glycogen phosphorylase (PYGL)

(A) Glycogen quantification in EV or shG6PC GBM1. (B) Representative western blot of pGYS1(Ser641), total-GYS1 and PYGL in EV or shG6PC GBM1. (C) Experimental design illustrating the time-points in which glycogen phosphorylase inhibitor CP-91149 (GPi) and 2DG were added to the groups depicted in figures D–J. (D) Representative images of cell invasion through the Boyden chamber from control, 2DG and recovery GBM1 treated with GPi or DMSO. (E–G) Comparison of the invasive capacity of EV or shG6PC in the presence or absence of GPi. (H–J) Cell viability and proliferation evaluated using alamarBlue in EV or shG6PC GBM1, in the presence or absence of GPi. The data are presented as the mean ± S.E.M (n=3) from three independent experiments. (*: $p<0.05$, **: $p<0.01$, ***: $p<0.001$).

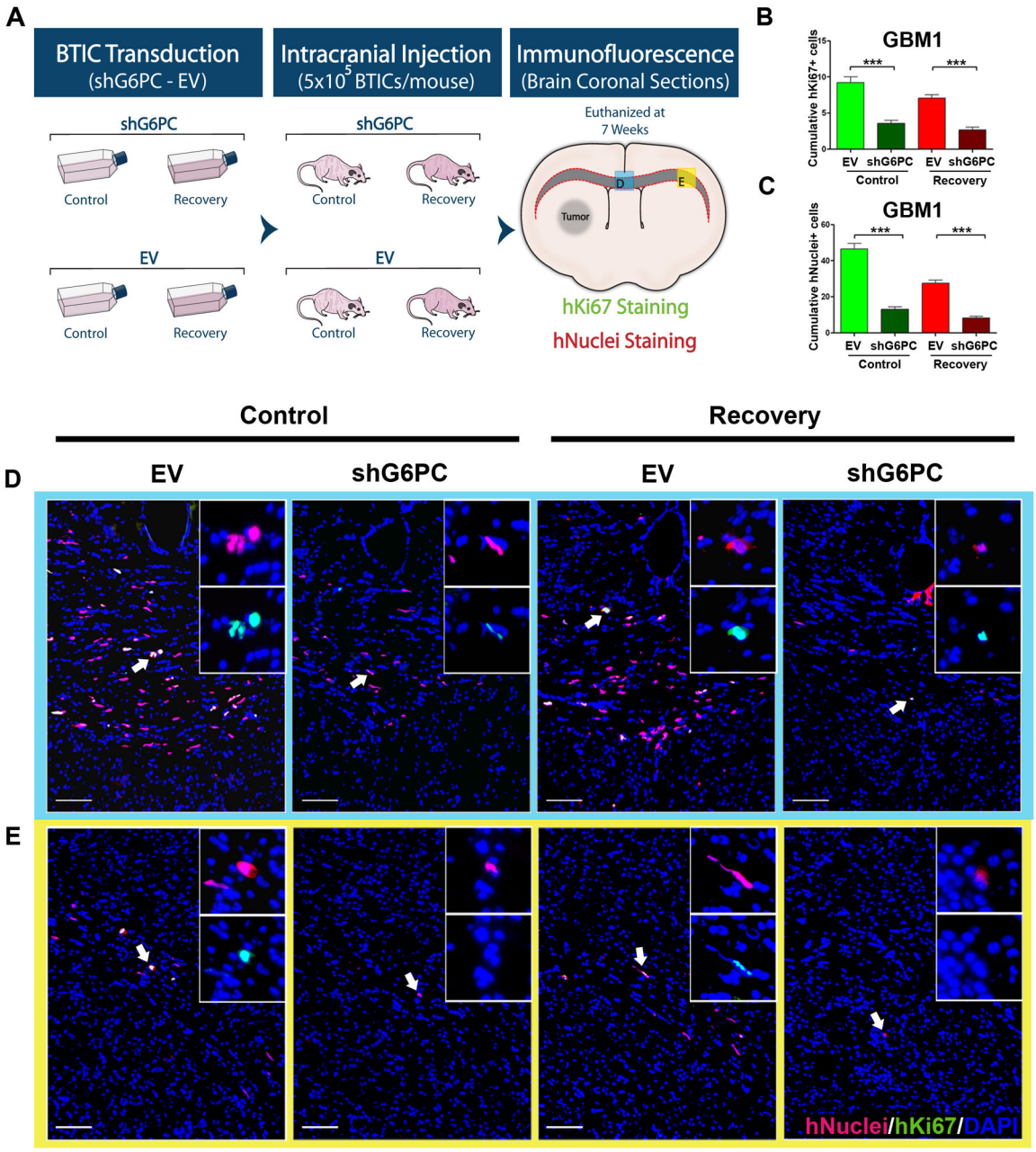

Figure 6. shG6PC reduces glioblastoma invasion *in vivo*.

(A) Schematization of the experimental design. GBM1 were transduced *in vitro* and injected intracranially into athymic nude mice. Mice were euthanized 7 weeks posterior to the injection and brain coronal sections were stained for human Ki67 and human Nuclei to evaluate proliferation and migration of BTICs through the corpus callosum. (B) Cumulative hKi-67 staining for proliferation across the corpus callosum. (C) Cumulative hNuclei staining across the corpus callosum. (D–E) Representative immunofluorescent images stained for hNuclei and hKi67. All Sections were acquired from the same two regions across the corpus callosum (labeled D and E in Figure 6A and outlined by the corresponding colors

in D and E). Values are expressed as mean ± SEM. positive cells/field. (***: p<0.001). Scale bars= 100 μm.

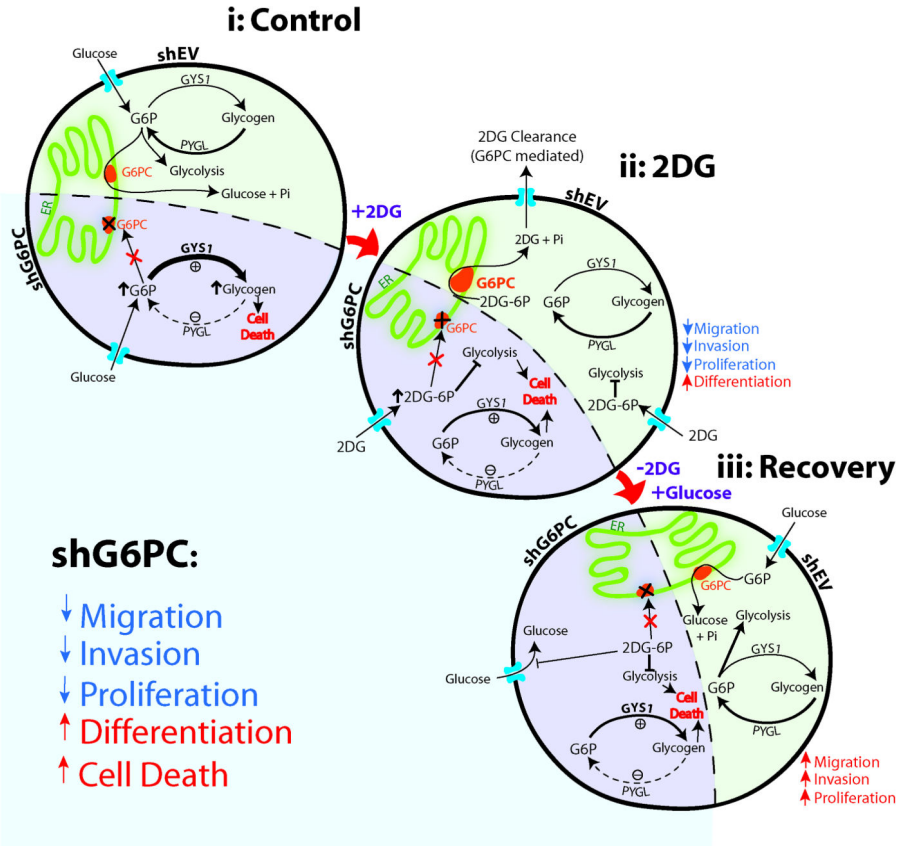

Figure 7. Summary of the hypothetical role of G6PC in BTIC response to glycolytic inhibition

G6PC is required for BTICs to counteract glycolytic inhibition with 2DG and regain the aggressive phenotype (invasion, migration and proliferation). shG6PC renders the majority of these cells unable to survive glycolytic inhibition. These changes occur through the activation of glycogen synthase (GYS1) and inhibition of glycogen phosphorylase (PYGL), which accumulates glycogen in the brain tumor cells and impairs their survival.